2018 21st International Conference on Intelligent Transportation Systems (ITSC)
Maui, Hawaii, USA, November 4-7, 2018

Design and Vehicle Implementation of Autonomous Lane Change Algorithm based on Probabilistic Prediction

Heungseok Chae, Yonghwan Jeong, Seonwook Kim, Hojun Lee, Jongcherl Park and Kyongsu Yi, *Member, IEEE*

***Abstract*— This paper describes design, vehicle implementation and validation of a motion planning and control algorithm of autonomous driving vehicle for lane change. Autonomous lane change is necessary for high-level autonomous driving. A vehicle equipped with diverse devices like sensors and computer is introduced for implementation and validation of autonomous driving. The autonomous driving system consists of three parts: perception, motion planning and control. In a perception part, surrounding vehicles' states and lane information are estimated. In motion planning part, using these information and chassis information, probabilistic prediction is conducted for ego vehicle and surrounding vehicle separately. And then, driving mode are decided among three modes: lane keeping, lane change and traffic pressure. Driving mode is determined based on a safety distance by predicting states of surrounding vehicles and ego vehicle. If the ego vehicle cannot perform lane change when the lane change is required, the most proper space is selected considering the probabilistic prediction information and the safety distance. Target states are defined based on driving mode and information of surrounding vehicles behaviors. In control part, the distributed control architecture for real time implementation to the vehicle. A linear quadratic regulator (LQR) optimal control and a model predictive control (MPC) are used to obtain the longitudinal acceleration and the desired steering angle. The proposed automated driving algorithm has been evaluated via vehicle test, which has used one autonomous vehicle and two normal vehicles.**

I. INTRODUCTION

Many driver assistance systems (ADAS) have been commercialized by automakers to enhance vehicle safety. In addition, autonomous driving systems in limited road environments have also been successfully developed by the use of advanced sensing technologies. Moreover, future developments will increase the highly autonomous systems with enhanced safety [1]. As next step of ADAS technology, the autonomous driving system has been researched worldwide. The autonomous driving system is generally integration of ADAS and controls longitudinal and lateral behavior of vehicle simultaneously. In longitudinal control, SCC and TJA control acceleration or deceleration to maintain set speed or guarantee safe clearance with front vehicle [2]. In lateral control, LKAS or LCAS generates assistant steering torque to conduct lane keeping or lane change procedure [3].

Autonomous lane change is necessary for the highly autonomous driving. This system is that, when a lane change is required, determines the availability of a lane change and then goes to the appropriate location and completes the lane change with keeping the surrounding vehicles safe. Therefore, since the autonomous lane change control requires both longitudinal and lateral control, it is difficult to implement. Previous researches for a lane change in autonomous driving systems shows diverse approaches. Simple model, cost function, human driver data and learning based approaches have been used to consider various factors for lane change [4-9]. Also, diverse model predictive control (MPC) is utilized ensuring the safety in finite time horizon [10-11]. However, no studies have yet been done for a motion planning and control for lane change considering both performance and computational power, which is important to vehicle implementation. Also, the studies are insufficient for the autonomous lane change covering the diverse traffic situations, including congested traffic flow.

In this study, using probabilistic prediction algorithms of ego vehicle and surrounding vehicle, the autonomous lane change algorithm have been designed ensuring safety and robustness with surrounding vehicles in the near future. In the motion-planning part, based on prediction information, the autonomous driving vehicle judges for possibility lane change, searches suitable space for lane change and decides the proper target states. However, under congested traffic situations, there can be no proper space for lane change. Therefore, the lane change intention should be transmitted to the side rear vehicle on target lane. In this paper, the concept of 'traffic pressure' has been introduced to transmit the lane change intention. The autonomous vehicle slightly sticks to the target lane to convey lane change intention.

In this paper, a control architecture is proposed for vehicle implementation. MPC is a very proper control technique with probabilistic prediction and has excellent performance. However, when MPC is used for all control values that are steering angle and longitudinal acceleration, the amount of calculation becomes too large. For real time implementation to vehicle, the distributed control architecture is adopted using linear quadratic Linear-Quadratic Regulator (LQR) of the longitudinal control and MPC of lateral control [12-13].

This paper is constituted as follows: the section II presents a test vehicle and an overall architecture of the proposed autonomous driving control algorithm. In Section III, probabilistic prediction algorithms of ego vehicle and

This research was supported by the Korea Ministry of Land, Infrastructure and Transport and the Korea Agency for Infrastructure Technology Advancement(Project No.: 18TLRP-B117133-03). This work was also supported by the Technology Innovation Program (10079730, Development and Evaluation of Automated Driving Systems for Motorway and City Road and driving environment) funded By the Ministry of Trade, Industry & Energy(MOTIE, Korea). This work was also supported by the National Research Foundation of Korea(NRF) grant funded by the Ministry of Science and ICT(NRF-2016R1E1A1A01943543).

H. Chae, H. Lee, J. Park and K. Yi are with the Seoul National University, Seoul, Korea (phone: +82-2-880-1941; fax: +82-2-888-7794; e-mail: kyi@snu.ac.kr)

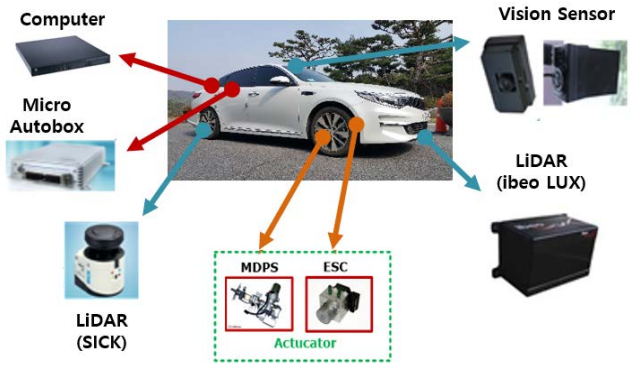

Fig. 1. Test Vehicle Configuration

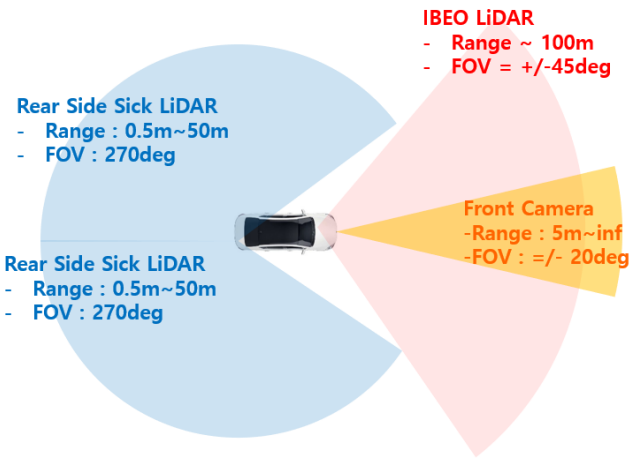

Fig. 2. Environment Sensor Range of Test Vehicle

surrounding vehicle are described. Then section IV, motion planning algorithm is described. In section V, LQR and stochastic MPC based lower-level controllers are designed. Then Section VI shows the vehicle test results to validate the proposed autonomous lane change algorithm. Finally, the conclusion of this research and the future works are in section VII.

II. Algorithm Architecture

A. Test Vehicle Configuration

In this study, test vehicle is equipped with close-to-production or commercialized sensors and a referencing system. For obstacle detection, one four-layer lidar is mounted on the front bumper. Also, on the back side, two single-layer lidar are installed. For lane detection, a monocular vision system was installed on the windshield. The RTK-DGPS is installed for only used for reference while conducting verification. Three lidars are interfaced using ethernet, and the other systems are interfaced using the control area network (CAN) bus and the discretized command signals are transmitted. The controller consists of a computer and Micro-Autobox. Final vehicle control is carried out using a commercialized ADAS system. The equipped test vehicle system is shown in Fig. 1. Fig. 2 shows sensor configuration which enables the all-around detection for changing lanes.

B. Overall System Architecture

In this research, overall automous driving algorithm consists of three layers is depicted in Fig.3. The perception block estimates environment. The most basic environment required for autonomous driving is information of lane and surrounding vehicle. Using extended Kalman filter, center lane is estimated by both lane information measured through front camera [14-15]. is Using point clouds measured by LiDAR sensors, vehicle detection accomplished through the following three steps: 1) clustering, 2) shape extraction, 3) extended Kalman filter [16]. And then, probabilistic prediction is conducted by perception and chassis information. In motion planning block, driving mode and target states are decided based on prediction information. The control block uses the environment and planned vehicle motion to optimize the steering and longitudinal acceleration input to the vehicle. In this paper, prediction, motion planning part and control part are mainly discussed.

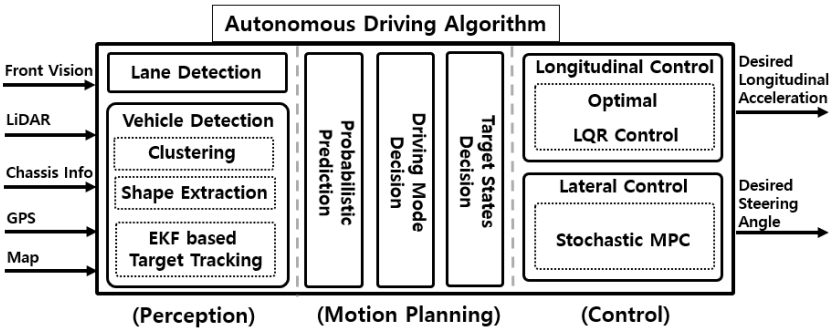

Fig. 3. Overall System Architecture

III. Probabilistic Prediction

A. Ego Vehicle Model & Prediction

As mentioned above, the distributed control architecture is adopted to obtain an advantage in computational power. Therefore, the longitudinal and lateral modeling are conducted separately. The longitudinal dynamics model is designed by considering both the longitudinal dynamics and the longitudinal actuator's dynamics. The actuator's dynamics is adopted of first order delay model. The state space model of the longitudinal dynamics can be written as Eqs. (1) and (2).

$$A_{long}=\begin{bmatrix}0 & 1 & 0\\ 0 & 0 & 1\\ 0 & 0 & -1/\tau_{ax}\end{bmatrix},\ B_{long}=\begin{bmatrix}0\\ 0\\ 1/\tau_{ax}\end{bmatrix} \tag{1}$$

$$\dot{\bar{x}}_{long}(t)=A_{lang}\bar{x}_{long}(t)+B_{long}u_{long}(t) \tag{2}$$

where, $\bar{x}_{long}=[p_x \quad v_x \quad a_x]^T$ and $u_{long}=a_{x,des}$ are state and input, respectively. p_x denotes the longitudinal position, v_x denotes longitudinal velocity, a_x denotes longitudinal acceleration and $u_{long}=a_{x,des}$ denotes longitudinal acceleration control input.

The lateral dynamics model is designed by integrating the bicycle model and error dynamics with a desired path of road [17-18].

$$A_{lat}=\begin{bmatrix} -\frac{2C_f+2C_r}{mv_x} & -\frac{-2C_fl_f+2C_rl_r}{mv_x} & 0 & 0 \\ -\frac{2C_fl_f+2C_rl_r}{I_z} & -\frac{2C_fl_f^2+2C_rl_r^2}{I_zv_x} & 0 & 0 \\ 0 & 1 & 0 & 0 \\ v_x & 0 & v_x & 0 \end{bmatrix}, B_{lat}=\begin{bmatrix} \frac{2C_f}{mv_x} \\ \frac{2C_fl_f}{I_z} \\ 0 \\ 0 \end{bmatrix}, F_{\rho,lat}=\begin{bmatrix} 0 \\ 0 \\ -v_x \\ 0 \end{bmatrix} \quad (3)$$

$$\dot{\bar{x}}_{lat}(t)=A_{lat}\bar{x}_{lat}(t)+B_{lat}u_{lat}(t)+F_{lat}\rho_{ref}(t) \quad (4)$$

where, $\bar{x}_{lat}=\begin{bmatrix}\beta & \gamma & e_\psi & e_y\end{bmatrix}^T$, $u_{lat}=\delta_f$ and ρ_{ref} are state, input and disturbance, respectively. β denotes tire-slip angle , γ denotes longitudinal velocity, e_ψ denotes the orientation error of the vehicle with respect to the road, e_y denotes the lateral offset with respect to the centerline of the lane, δ_f denotes the desired steering angle control input and ρ_{ref} is the road curvature measured by vision sensor.

Prediction is proceeded according to the each model. The input used is the trajectory of desired longitudinal acceleration and desired steering angle determined in the control part. Prediction horizon is 2sec and prediction sampling time is 0.1sec. Eqs. (5) and (6) shows prediction equations. t and k represent the current time and the prediction step, respectively.

$$\bar{x}_{long}(t+k+1)=A_{lang}\bar{x}_{long}(t+k)+B_{long}u_{long}(t+k) \quad (5)$$

$$\bar{x}_{lat}(t+k+1)=A_{lat}(t+k)\bar{x}_{lat}(t+k)+B_{lat}(t+k)u_{lat}(t+k) + F_{lat}(t+k)\rho_{ref}(t+k) \quad (6)$$

To identify the bounded disturbance of each states, Disturbance analysis is conducted based on experimental data. The one-step state prediction using the system model is compared with the current measured data. Probabilistic uncertainty propagation of each states is achieved [19].

B. *Surrounding Vehicles Prediction*

Along with ego vehicle prediction, the autonomous driving system needs to predict surround vehicles prior to the motion planning and control. Vehicle detection module perceives surrounding vehicle's behavior by LiDAR sensor. Surrounding vehicle's behavior is predicted to guarantee safety in foreseeable future.

For the prediction of the reasonable and realistic behaviors of surrounding vehicles, the interaction between vehicles and the restriction on surrounding vehicles due to the road geometry should be considered. It is assumed that drivers of the surrounding vehicles follow traffic rules. In setting reasonable ranges of the future states of surrounding vehicles, driving data is collected on a test track and real road to analyze the probabilistic movement characteristics of the vehicle. Two parts can be divided in the probabilistic prediction algorithm. The first part is vehicle state predictor, using estimated states of surrounding vehicle as current states. For prediction, future control inputs are needed: longitudinal acceleration and steering angle. Longitudinal acceleration is assumed in decayed from current acceleration to zero. Steering angle is decided in next part. The second part is a path-following model that generates the future desired yaw rate. A path-following model is designed to implement these assumptions while interacting with a vehicle state predictor during one cycle of the prediction process. In a vehicle state predictor, the vehicle's reasonable position and its error covariance are predicted by Extended Kalman Filter using the desired yaw rate obtained by the path-following model as the virtual measurement [20-21].

Fig. 4 depicts the overall architecture of probabilistic prediction of surrounding vehicles. Using measurements from the various sensors, such as vehicle sensor, radar and vision sensor, the range of the predicted states with corresponding uncertainty is determined as shown in Fig. 4. t_k denotes the length of the prediction horizon, and subscript 'j' means the j-the surrounding vehicles. In predicting the position of the surrounding vehicle, it is assumed that the size of the surrounding vehicle is equivalent to the subject vehicle.

IV. Motion Planning Algorithm

In this section, desired motion is decided based on probabilistic prediction information as mentioned above. Firstly, the autonomous vehicle determines a driving mode: lane keeping or lane change. To cope with a congested traffic, a traffic pressure mode was also devised. And then, the desired motion is planned based on safety with the surrounding vehicles and the determined driving mode. The desired motion

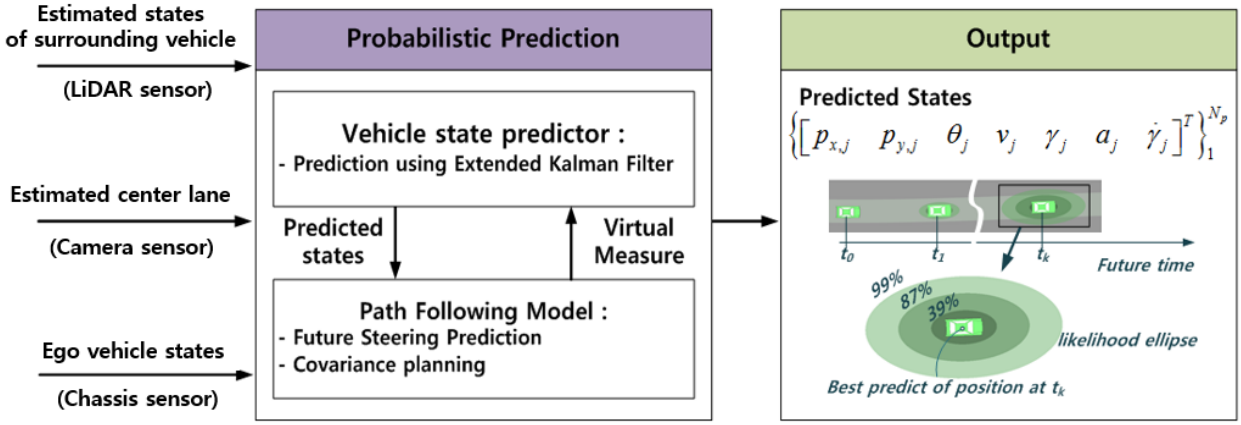

Fig.4. Overall architecture of probabilistic prediction of surrounding vehicle's behavior

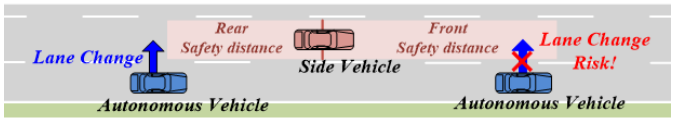

Fig. 5. Lane Change Risk based on Safety Distance

is defined both longitudinally and laterally.

A. Driving Mode Decision

Most of the autonomous driving vehicle's driving situation is lane keeping driving. If there is a preceding vehicle, the autonomous driving vehicle follows the preceding vehicle. However, if the preceding vehicle is too slow or the autonomous vehicle is located at merge or split section, then the lane change is necessary. In this paper, when a lane change is required in the above situations, the lane change mode and the lane keeping mode are determined through lane change risk monitoring. The lane change risk is determined by a safety distance to the vehicles on the target lane that are aimed at lane change [22]. The safety distance is expressed in Eq. (7). Depending on whether the side vehicle is located at the front or rear, the safety distance is different. A greater safety distance should be required when the speed of the rear vehicle is faster than the front.

$$\begin{aligned} SD_{front,j}(t) &= \max\left\{\left(v_{x,j}(t)-v_{x,ego}(t)\right),0\right\}\cdot\tau_{SD}+c_{SD}+\sigma_{ego}(t)+\sigma_{side}(t) \\ &\quad (if\ p_{x,j}>0) \\ SD_{rear,j}(t) &= \max\left\{\left(v_{x,ego}(t)-v_{x,j}(t)\right),0\right\}\cdot\tau_{SD}+c_{SD}+\sigma_{ego}(t)+\sigma_{side}(t) \\ &\quad (elseif\ p_{x,j}<0) \end{aligned} \tag{7}$$

where, $v_{x,ego}$ is the velocity of autonomous vehicle. $v_{x,j}$ is the velocity of j-th surrounding vehicle on target lane. τ_{SD} is the time gap about the relative velocity. c_{SD} is the minimum clearance. σ_{ego} is the position uncertainty of ego vehicle. σ_{side} is the position uncertainty of side vehicle. $p_{x,j}$ is the position of j-th surrounding vehicle. As the vehicle located at behind is different according to $p_{x,j}$, a different safe distance is applied.

If any of vehicles on the target lane is located closer to the safety distance within the prediction horizon, it is determined that there is lane change risk. Fig. 5 Present the lane change risk monitoring concept. And Eq. (8) expresses lane change risk condition. If lane change risk is detected only once in prediction horizon, lane change is impossible.

$$\begin{aligned} &If\ \Delta p_{x,j}(t+k) < [SD_{front,j}(t+k) \parallel SD_{rear,j}(t+k)] \\ &\quad Lane\ Change\ Risk! \\ &end \end{aligned} \tag{8}$$

where, Δp_x is relative longitudinal positon between ego and surrounding vehicle, SD_{front} denotes the front lane change safety distance, and SD_{rear} denotes the rear lane change safety distance. What is compared with and depends on whether the surrounding vehicle is in front or behind.

When there is the lane change risk, proper longitudinal motion planning is needed. In Fig. 6 (a), there are several space candidates that is based on the safety distance. Space candidates are defined Eq. (9). Through probabilistic prediction of ego vehicle and surrounding vehicles, target space is decided among possible spaces. In Fig. 6 (b), there is not possible space for lane change under congested traffic situations, because all safety distances are overlapped. In this case, the lane change intention should be transmitted to the side rear vehicle on target lane. In this paper, the concept of 'traffic pressure' has been introduced to transmit the lane change intention. As shown in Fig. 7, traffic pressure means that the autonomous vehicle is keeping the original lane sticking to the target lane slightly. As a conclusion, there are three driving modes depending on the safety distance: lane keeping, lane change and traffic pressure. In traffic pressure mode, possible space candidates are determined by not safety distance but vehicle length. Desired space candidates are defined as Eq. (10).

$$\begin{aligned} p_{LC\,cand\,front,j}(t+k) &= p_{x,j}(t+k)+SD_{front,j}(t+k) \\ p_{LC\,cand\,rear,j}(t+k) &= p_{x,j}(t+k)-SD_{rear,j}(t+k) \end{aligned} \tag{9}$$

$$\begin{aligned} p_{LC\,cand\,front,j}(t+k) &= p_{x,j}(t+k)+L_{vehicle} \\ p_{LC\,cand\,rear,j}(t+k) &= p_{x,j}(t+k)-L_{vehicle} \end{aligned} \tag{10}$$

To select the desired space among candidates, prediction information is utilized. a cost is calculated as shown in Eq. (11). For the cost are used two indexes that are possible space candidate 'j' and prediction acceleration candidate 'k'. For cost calculation, the ego vehicle is assumed to have acceleration in the range $2m/s^2$ to $-2m/s^2$. This range may vary depending on the presence of preceding vehicle or the maximum speed limit. The prediction horizon is the allowed time horizon for lane change like remained time at the merge section. The cost is consist of three terms. Firstly, a cost time is the minimum time that the ego vehicle reach to a desired space candidate in the prediction horizon. Secondly, a cost velocity is relative velocity between surrounding vehicle, which is related in space candidate, and ego vehicle at the cost time. Thirdly, a cost clearance is the clearance between adjacent space candidates at the cost time. The space, which has the minimum cost, is decided the final desired space. Consequently, the driving mode, which can be lane keeping, lane change and traffic pressure, and desired space for lane

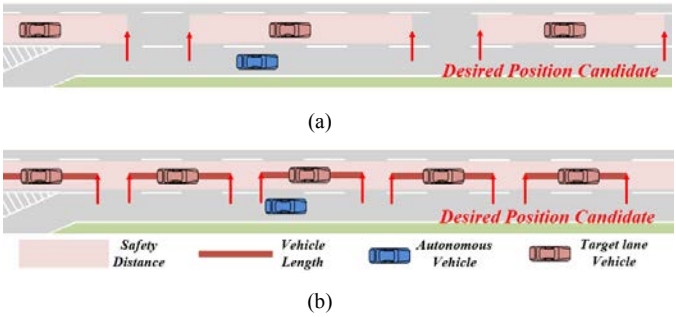

Fig. 6. Desired Space Candidates for Lane Change

Fig. 7. Traffic Pressure Concept

change are determined in diving mode decision.

$$J(j,k) = k_1 \cdot (t_{cost}(j,k)/t_{prediction}) + k_2 \cdot (v_{cost}(j,k)/v_{x,ego}) + k_3 \cdot (1/C_{cost}(j,k)) \quad (11)$$

B. Target State Decision

In the longitudinal target state decision, reference and constraint about position and velocity are determined. Basically, it is determined by the velocity limit and the driving mode. As shown Fig. 8, the target vehicle of interest is determined depending on the lane change sequence. When lane change is not possible although it is required, it is important that the desired space is determined based on the cost. During a lane change, the preceding vehicle is important. The same applies when the lane change is completed, which is identical with the lane keeping mode.

In lateral target state decision, reference and constraint about lateral position are determined. According to three modes as described above, reference is decided as expressed in Eq. (12). It is essential to track center path in lane keeping mode. In lane change mode, a hyperbolic tangent path is suggested for low acceleration jerk. Traffic pressure mode has a reference that slightly sticks to the target lane. Constraint is determined as a safe driving area based on the predicted behavior of all surrounding vehicles.

$$e_{y,ref}(t) = \begin{cases} 0 & \text{in Lane Keeping Mode} \\ \pm\frac{W_{road}}{2} \mp \varepsilon_y & \text{in Traffic Pressure Mode} \\ C_1 \cdot \tanh(C_2 \cdot t + C_3) + C_4 + e_{y,0} + L_p & \text{in Lane Change Mode} \end{cases} \quad (12)$$

where, W_{road} denotes road width, ε_y denotes offset for traffic pressure, $e_{y,0}$ is lateral position error of current time, L_p is preview distance, C_1, C_2, C_3 and C_4 is constant value for lane change described in detail in [19].

V. Vehicle Control

In the control algorithm section, the distributed control system is introduced. This system enables to reduce calculation time and ensure minimum performance. If SMPC is used for both longitudinal control and lateral control, the calculation time is greatly increased. Thus, the longitudinal control uses the LQR control, because it can be relative less sophisticated. In the lateral control, especially in the lane change control, the stochastic model predictive control is used for ensuring good performance even at the expense of computation time.

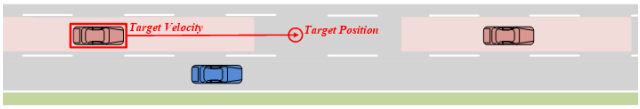

(a) Before lane change

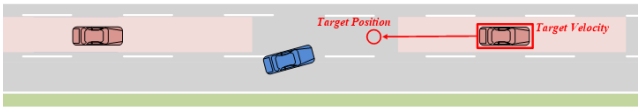

(b) During lane change

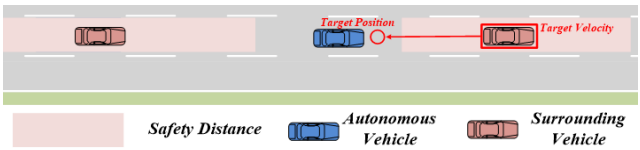

(c) After lane change / lane keeping

Fig. 8. Longitudinal target states decision

A. Longitudinal Control: LQR Control

The desired acceleration is determined by the longitudinal target states. The linear optimal problem is formulated based on the longitudinal vehicle model. As shown in (13), the final input is calculated using $\bar{k}$ obtained by (14).

$$a_{x,des}(t+k) = u_{long}(t+k) = -\bar{k}(\bar{x}_{long}(t+k) - \bar{x}_{long,des}(t+k)) \quad (13a)$$

$$s.t.\ \ u_{longi,\min} \le u_{longi}(k|t) \le u_{longi,\max} \quad (13b)$$

$$(k = 0, \ldots, N_{p-1}) \quad (13c)$$

$$J = \int_0^{\infty} \left(x_{long}{}^T Q_{long}\ x_{long} + u_{long}{}^T R_{Long}\ u_{long} \right) dt \quad (14a)$$

$$s.t.\ \ \bar{x}_{long}(t+k+1) = A_{lang}\bar{x}_{long}(t+k) + B_{long}u_{long}(t+k) \quad (14b)$$

where, Q_{long} and R_{long} denote weighting matrices; t is the current time instant; $\bar{x}_{long}(t+k)$ is the predicted subject vehicle longitudinal state at time $t+k$ derived by applying the control sequence $u_{long}(t+k)$ to the vehicle model Eq. (14b). and Eqs. (13b) is control input constraints, $u_{longi,\min}$ is -2 m/s^2, and $u_{longi,\max}$ is 2 m/s^2.

B. Lateral Control: Stochastic Model Predictive Control

SMPC problem used to calculate the desired control inputs for control performance. The SMPC problem is formulated using the vehicle dynamics model, the lateral target states and constraints of states and input. The SMPC is solved to determine a sequence of control inputs that are applied to the system as follows [19]:

$$\min \sum_{k=0}^{N_p-1} \mathbb{E}\left(\left\| \bar{x}_{lat}(t+k+1|) - \bar{x}_{lat,des}(t+k+1) \right\|_{Q_{lat}}^2 + \left\| u_{lat}(t+k) \right\|_{R_{lat}}^2 \right) \quad (15a)$$

$$s.t.\ \ \bar{x}_{lat}(t+k+1) = A_{lat}(t+k)\bar{x}_{lat}(t+k) + B_{lat}(t+k)u_{lat}(t+k) + F_{lat}(t+k)\rho_{ref}(t+k) \quad (15b)$$

$$\Pr\left(g^T(k+1)x(k+1) \le h(k+1) \right) \ge 1 - \varepsilon(k) \quad (15c)$$

$$\left| u_{lat}(t+k) \right| \le u_{lat,\lim} \quad (15d)$$

$$\left\| u_{lat}(t+k+1) - u_{lat}(t+k) \right\|_{\infty} \le S_{lat} \quad (15e)$$

$$(k = 0, \ldots, N_{p-1}) \quad (15f)$$

where, Q_{lat} and R_{lat} denote weighting matrices; t is the current time instant; $\bar{x}_{lat}(t+k)$ is the predicted subject vehicle longitudinal state at time $t+k$ derived by applying the control

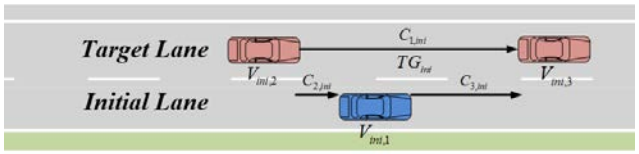

Fig. 9. Three Vehicles Relation of Test Scenario

sequence $u_{lat}(t+k)$ to the vehicle model Eq. (15b). And Eqs. (15d) and (15e) are control input constraints, $u_{lat,\lim}$ is 30 deg.

VI. Vehicle Test

The proposed autonomous driving algorithm is validated through vehicle test. As shown in Fig. 9, there are two normal vehicles on the first lane and an autonomous lane on the second lane. At this time, the autonomous driving vehicle is required to make a lane change to the left. The test scenarios are summarized in Tab. 1. There are four scenarios in total and the initial speed and initial position of the three vehicles are different. Especially, the scenario 4 assumes that virtual vehicles exits closely in front of and behind both side vehicles in order to simulate a congestion situation. The target speed of the autonomous vehicle is the same as the initial speed.

TABLE I. Initial Condition of Test Scenarios

No.	Initial Condition						
	$V_{ini,1}$	$V_{ini,2}$	$V_{ini,3}$	$C_{1,ini}$	$C_{2,ini}$	$C_{3,ini}$	TG_{ini}
1	30kph	30kph	30kph	10m	-10m	-20m	1.2
2	30kph	30kph	30kph	10m	-2m	12m	1.2
3	10kph	10kph	10kph	25m	-4m	21m	9.3
4	10kph	10kph	10kph	18m	-8m	10m	6.6

where, $V_{ini,1}$, $V_{ini,2}$ and $V_{ini,3}$ denote the initial velocity of the autonomous vehicle, rear-side vehicle and front-side vehicle. $C_{ini,1}$ denotes initial distance between rear-side vehicle and front-side vehicle. $C_{ini,2}$ denote the initial distance between the autonomous vehicle and rear-side vehicle. $C_{ini,3}$ denotes the initial distance between the autonomous vehicle and front-side vehicle. TG_{ini} denotes time-gap of rear-side vehicle to rear-front vehicle.

Fig. 10 shows four snap shots of each test scenario. The blue vehicle is the autonomous vehicle and the red vehicles are the surrounding vehicles. The blue line is the target path of autonomous vehicle, and the blurred blue vehicles are the predicted information after one and two seconds, respectively. Red points are point cloud of LiDAR sensor. On the right side of the autonomous vehicle, guardrails and trees are recognized by LiDAR. On the left side, the corners of the surrounding vehicles are recognized by LiDAR and perceived as vehicles by the perception algorithm. The long rectangular box around the red vehicle indicates the safe distance used in the motion planning algorithm. The green line indicates the lanes recognized by the camera sensor, and the black dotted line is the centerline of the lanes processed by the lane filter.

The first snapshot in each scenario shows the initial condition. In all scenarios, although a lane change is required, there is a lane change risk due to safety distance of the side vehicles on the target lane. The second snapshots shows the autonomous driving vehicle taking action to be able to change lanes. In scenario 1, the autonomous vehicle determines that it is best to move in front of the side-front vehicle, and accelerate. In scenario 2, the autonomous vehicle determines that it is best to move behind the side-rear vehicle, and decelerates. In scenario 3, the autonomous vehicle judges that there is sufficient space between the side-rear vehicle and the side-front vehicle and accelerates to enter that space. As mentioned above, the scenario 4 assumes that virtual vehicles exits closely in front of and behind both side vehicles in order to simulate a congestion situation. Therefore, the autonomous vehicle does not judge that it is good to move at the most forward or the rearmost point like scenario 1, 2. The autonomous vehicle proceeds with traffic pressure to convey the lane change intention to the side-rear vehicle. In other words, the autonomous vehicle goes into space between two side vehicles and attaches slightly to the target lane. The third snapshots shows the autonomous driving vehicle performing the lane change. Especially, in scenario 4, the side-rear vehicle responded to traffic pressure, giving space for lane change. The fourth snapshots shows that the lane change has been successfully completed while keeping the safety with the surrounding vehicles.

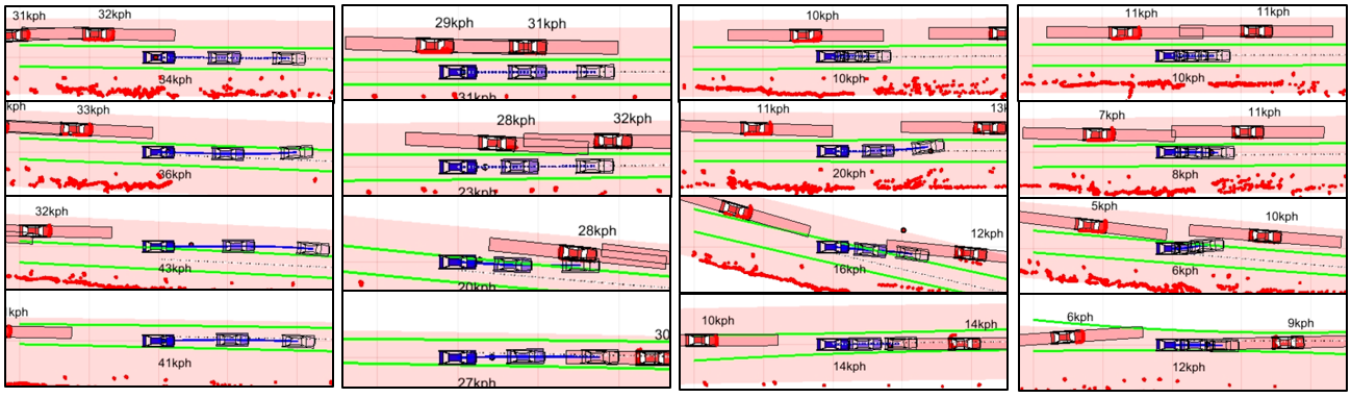

(a) Scenario. 1 (b). Scenario. 2 (c). Scenario. 3 (d). Scenario. 4

Fig. 10. Four Snap Shots of Each Test Scenarios

Fig. 11 shows test results of scenario 3. Fig. 11 (a) shows the longitudinal acceleration. From 0 to 8 seconds, the autonomous vehicle accelerates to a space where lane change is possible. The vehicle makes longitudinal control considering the safety with the side-front vehicle from 8 seconds, when the lane change starts. Fig. 11 (b) demonstrates, through lateral position by measured camera sensor, that the lane change starts from 8 seconds and the autonomous vehicle arrives at the target lane about 11 seconds. Fig. 11 (c) shows the steering angle used to performing lane change, demonstrating that the lane change is completely on the target lane at about 16 seconds. Fig. 11 (d) demonstrates domain of clearance and relative velocity with the side-front and side-rear vehicles. Black dots are before lane change. Red circles are during and after lane change. Initially, the side-rear vehicle is so close that the lane change cannot be performed. After the distance from the side-rear vehicle is extended, the lane change begins. This shows that the autonomous vehicle maintains the safety with surround vehicles when lane changing.

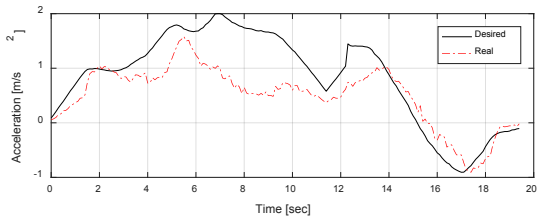

(a) Longitudinal acceleration

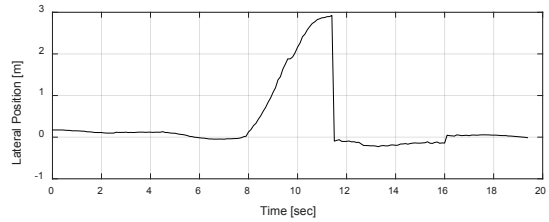

(b) Lateral position

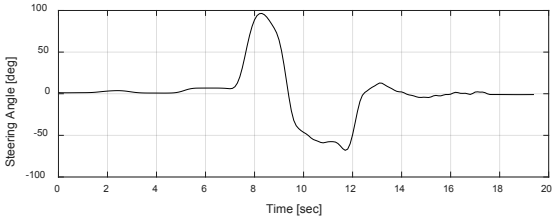

(c) Steering angle

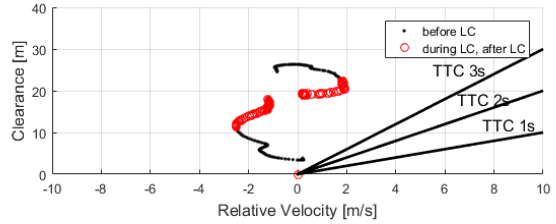

(d) Safety with surrouding vehicles

Fig. 11. Test reults of scenario 3

VII. Conclusion

The autonomous driving algorithm has been developed in this paper. This algorithm is mainly designed for autonomous lane change. A vehicle equipped with diverse devices like sensors and computer is introduced for autonomous driving. The autonomous driving system consists of three parts: perception, motion planning and control. Especially, motion planning and control parts are mainly discussed. In motion planning part, using these information and chassis information, probabilistic prediction is conducted for ego vehicle and surrounding vehicle separately. And then, driving mode are decided among three modes: lane keeping, lane change and traffic pressure. Traffic pressure mode is specially devised for the congested traffic that is difficult environment for lane change. Driving mode is determined based on a safety distance by predicted states of surrounding vehicles and ego vehicle. The safety distance considers relative velocity and relative position of subject and surrounding vehicles. If the ego vehicle cannot perform to lane change when the lane change is required, the most proper space is selected considering the probabilistic prediction information and the safety distance. Target states, which used for control reference and constraints, are defined based on driving mode and information of surrounding vehicles behaviors. In control part, the distributed control architecture for real time implementation to the vehicle. A linear quadratic regulator (LQR) optimal control is used to obtain the longitudinal acceleration. While, the controller is designed to obtain the desired steering angle using a model predictive control (MPC) with constraints. The proposed automated driving algorithm has been evaluated via vehicle test, which has used one autonomous vehicle and two normal vehicles.

Future works aim at upgrading autonomous driving system. For the more enhanced autonomous driving, the requirement for lane change shall be determined automatically. Lane change is required when the preceding vehicle is too slow or the ego is located at the merge section. For this, a system with map information and localization module is required. In addition, it is necessary to carry out an analysis of the actual driving data and the characteristics of the vehicle to advance the algorithm. From this, algorithms can be developed to simulate the actual driving as well as the safety performance and to relieve the driver of this sensation. Future works also aim at testing the proposed control algorithm by driving on actual highway roads beyond vehicle test of limited road.

References

[1] E, Azim, *Handbook of Intelligent Vehicles*, London: Springer, 2012.

[2] K. Yi, and I. Moon, "A driver-adaptive stop-and-go-cruise control strategy," Networking, Sensing and Control, 2004 IEEE International Conference on, Vol. 1, Mar. 2004, pp. 601-606.

[3] Liu, W., Song, C., Fu, P., Wang, N., and Yuan, H, "A Rear Vehicle Location Algorithm for Lane Change Assist," MVA, 2007, pp. 82-85.

[4] Wan, Liming, et al. "Lane change behavior modeling for autonomous vehicles based on surroundings recognition," International Journal of Automotive Engineering 2.2: 7-12, 2011.

[5] J. Wei, J. Dolan, and B. Litkouhi, "A Prediction- and Cost Function-Based Algorithm for Robust Autonomous Freeway Driving," IEEE Intelligent Vehicle Symposium, 2010

[6] Wan, L., Raksincharoensak, P., Maeda, K., Nagai, M. "Lane Change Behavior Modeling for Autonomous Vehicles Based on Surroundings

Recognition", International Journal of Automotive Engineering, 2011, pp 7-12.

[7] Do, Quoc Huy, et al. "Human drivers based active-passive model for automated lane change," IEEE Intelligent Transportation Systems Magazine 9.1: 42-56, 2017.

[8] D. Kasper, G. Weidl, T. Dang, G. Breuel, A. Tamke, A. Wedel, and W. Rosenstiel, "Object-Oriented Bayesian Networks for Detection of Lane Change Maneuvers," ITS Magazine, vol. 4, no. 1, 2012.

[9] R.S. Tomar, S. Verma, G.S. Tomar, "Prediction of lane change trajectories through neural network," in Proc of International Conference on Computational Intelligence and Communication Networks, 2010, pp. 249 – 253.

[10] Yoshida, Hidehisa, Shuntaro Shinohara, and Masao Nagai. "Lane change steering manoeuvre using model predictive control theory," Vehicle System Dynamics 46.S1: 669-681, 2008.

[11] Cesari, Gianluca, et al. "Scenario Model Predictive Control for Lane Change Assistance and Autonomous Driving on Highways," IEEE Intelligent Transportation Systems Magazine 9.3: 23-35, 2017.

[12] Camacho, Eduardo F., and Carlos Bordons Alba. *Model predictive control*. Springer Science & Business Media, 2013.

[13] Bemporad, Alberto, et al. "The explicit linear quadratic regulator for constrained systems," Automatica 38.1: 3-20, 2002.

[14] Kalman, Rudolph Emil. "A new approach to linear filtering and prediction problems," Journal of basic Engineering 82.1: 35-45, 1960.

[15] Khosla, Deepak. "Accurate estimation of forward path geometry using two-clothoid road model," Intelligent Vehicle Symposium, IEEE. Vol. 1, 2002.

[16] D. Streller, K. Furstenberg, and K. Dietmayer, "Vehicle and object models for robust tracking in traffic scenes using laser range images," in Intelligent Transportation Systems, Proceedings. The IEEE 5th International Conference on, 2002, pp. 118-123.

[17] Falcone, Paolo, et al. "Predictive active steering control for autonomous vehicle systems," IEEE Transactions on control systems technology 15.3: 566-580, 2007

[18] Enache, N. Minoiu, et al. "Driver steering assistance for lane departure avoidance," Control engineering practice 17.6: 642-651, 2009.

[19] S, Jongsang, H. Chae, and K. Yi, "Stochastic Model Predictive Control for Lane Change Decision of Automated Driving Vehicles," IEEE Transactions on Vehicular Technology, 2018.

[20] K. Beomjun, and K. Yi, "Probabilistic states prediction algorithm using multi-sensor fusion and application to Smart Cruise Control systems," Intelligent Vehicles Symposium (IV), IEEE, 2013.

[21] K. Beomjun, and K. Yi, "Probabilistic and holistic prediction of vehicle states using sensor fusion for application to integrated vehicle safety systems," IEEE Transactions on Intelligent Transportation Systems 15.5: 2178-2190, 2014.

[22] H. Chae, K. Min, and K. Yi, "Model Predictive Control based Automated Driving Lane Change Control Algorithm for Merge Situation on Highway Intersection," No. 2017-01-1441. SAE Technical Paper, 2017.